ChemElectroChem

Research Article
doi.org/10.1002/celc.202300525

Chemistry Europe
European Chemical Societies Publishing

www.chemelectrochem.org

Broadening Applicability of the Poor Academic's Method for Reversing Polarity in Redox Flow Cell Cycling

Gimena Marin-Tajadura,[a, b] Eduardo Sánchez-Díez,[c] Virginia Ruiz,*[a, b] and Edgar Ventosa*[a, b]

The use of symmetrical cells is becoming popular for the search of new electroactive materials in redox flow batteries. Unfortunately, low-cost battery cyclers, commonly used for electrochemical battery testing, are not compatible with symmetrical cells since they usually cannot apply negative bias voltages needed for symmetrical cells. The insertion of a Ni–Cd battery in the voltage sensing path is a simple and effective methodology to overcome this limitation for certain battery cyclers. Herein, the validity of this useful method is evaluated for other battery cyclers, realizing that the strategy is not universal. A modified methodology is developed for a battery cycler in which the previous method is not valid. The new strategy is based on inserting a Ni-MH battery in the current path, and enables using a low-cost Neware CT-4008T-5V6A-S1 cycler for ferro- /ferricyanide symmetrical cells demonstrating proper operation for >19 days. This new method possesses advantages, e.g. direct reading of the cell voltage, and disadvantages, e.g. the Ni-MH battery is charged/discharged during operation, which are discussed. The four battery cyclers evaluated show that, despite neither method is universal, both methods are complementary to each other. Thus, the decision of using either one method or the other must be reached on a case-by-case basis.

Introduction

Redox Flow Batteries (RFBs) are a family of battery technologies, which are featured by the fact that the energy storing species are stored in reservoirs outside the electrochemical reactor.[1] This intrinsic characteristic of RFBs enables independent scalability of energy and power, which represents a great asset for middle-, long- term energy storage and make RFBs promising candidates for large-scale energy storage systems for the electric grid.[2] For stationary energy storage applications, cost and lifespan are critical parameters.[3] The all-vanadium flow battery (AVRFB) is the state of the art RFB.[4] While the lifespan of AVRFB fulfils the requirements for stationary energy storage, cost of vanadium (critical material for the USA[5] and Europe[6]) is fluctuating, which has triggered high interest in the search for more sustainable active species.[7] One of the most important parameters that the alternative active species must fulfill is to possess a long lifespan.[8] However, evaluation of the intrinsic stability of new active species is not always straightforward, since (electro-) chemical stability of active species is not the only source for energy storage capacity fading.[9] Symmetric flow cells, with identical composition on both sides, are used to investigate capacity fade of active species in RFB minimizing contribution from crossover of redox active species.[10] In the case of exploring new catholytes, Faradaic imbalance, driven by the presence of small amounts of oxygen in the anolyte,[11] also interferes with the evaluation of intrinsic stability of the catholyte, in which cases symmetric flow cells are also very convenient.[12] The advantages of symmetric flow cells for evaluating cycling stability has been also seized in other type of flow batteries, such as the redox-mediated flow battery, facilitating investigation of the stability for charge transfer between the redox mediator and the solid booster.[13] Cycling symmetric flow cells requires that battery cyclers are capable of applying negative bias voltages. However, common battery cyclers can only apply bias voltages over positive ranges. In this regard, Aziz's group recently reported a simple yet very useful methodology to extend the accepted voltage range of a battery cycler to negative bias voltages.[14] It consists on adding manually a DC-offset, achieved by a constant voltage source incorporated externally from the battery cycler, to the signal sensed by the instrument tricking the system into imposing on the battery the desired bias voltage, which may be outside of the cycler's voltage range capability. This pioneering work was implemented and validated using a top-range Novonix cycler. Although battery cycler manufacturers rarely disclose the details of the electronic components and design, it is likely to assume that there are significant differences in the electronics

[a] G. Marin-Tajadura, Dr. V. Ruiz, Dr. E. Ventosa
International Research Center in Critical Raw Materials-ICCRAM
Universidad de Burgos
Plaza Misael Bañuelos s/n, E-09001, Burgos (Spain)
E-mail: vrfernandez@ubu.es
eventosa@ubu.es

[b] G. Marin-Tajadura, Dr. V. Ruiz, Dr. E. Ventosa
Departamento de Química, Facultad de Ciencias
Universidad de Burgos
Pza. Misael Bañuelos s/n, E-09001-Burgos (Spain)

[c] Dr. E. Sánchez-Díez
CIC Energigune
Albert Einstein, 48, E-01510 Vitoria-Gasteiz (Spain)

Supporting information for this article is available on the WWW under https://doi.org/10.1002/celc.202300525

among different brands. Thus, the desired applicability of this ingenious strategy to other battery cyclers remains an open question.

In this work, it is shown that the methodology is not suitable for a lower-range battery cycler, i.e. a Neware BTS battery testing system CT-40087-5V6A-S1. Although the battery cycler suppliers do not provide information about the instrument internal configuration/circuitry, it is reasonable to assume that the limitation arises from the different electronics. In the previous reported method for reversing polarity in electrochemical cell testing, a nickel-cadmium battery was incorporated in the path of the battery cycler's voltage sense, tricking the instrument into accepting the user's desired applied voltage. In this work, it is proposed an adaptation of the original experimental setup that allowed reversing polarity during redox flow cell cycling in those battery cyclers where the original method failed to work. Specifically, the setup incorporates a nickel metal hydride (Ni-MH) battery in the path of the current providing an alternative solution to the limitation of certain battery cyclers to apply negative voltages. Advantages and limitations of this approach related to the state of charge of the Ni-MH battery are disclosed, and its suitability for long-term cycling of symmetric redox cells under static and flow configuration using both galvanostatic or potentiostatic methods is demonstrated.

Results and discussion

Demonstration of the modified set-up operation

We initially tested the applicability of the reported DC-offset method for galvanostatic cycling of a low-volume (0.45 mL in each side) static ferro/ferricyanide symmetric cell using a Neware CT-4008T-5V6A-S1 cycler. A Ni-MH battery (1.2 V, 1.18 Ah) was incorporated in the path of the voltage sense circuit to add the battery voltage value to the sensed cell voltage difference, thus tricking the cycler into accepting the measured voltage (Figure 1b). The cell was composed of 0.2 M ferro-/0.3 M ferricyanide in 1 M KCl as single electrolyte for positive and negative sides. It was operated galvanostatically at current densities of $\pm 15\ mA\,cm^{-2}$ with cut-off voltage values of ± 0.45 V both without and with the manual DC-offset. As expected, it was not possible to discharge the cell without the DC-offset since the cycler does not have negative voltage capability (Figure 1a). Unfortunately, the same limitation was encountered when the manual DC-offset was introduced by incorporating a Ni-MH battery with an OCV of 1.2 V in the path of the cell working electrode voltage sense leads, as proposed by Aziz et al.[14] (Figure 1b). This experiment shows that the manual DC-offset is not a universal strategy for reversing polarity applicable to all battery cyclers. As indicated above, the limitation likely originates from a limitation of the hardware rather than the software, as likely the power supply of the Neware cycler used is not capable of applying negative voltage values (the sensing path is used to monitor the voltage).

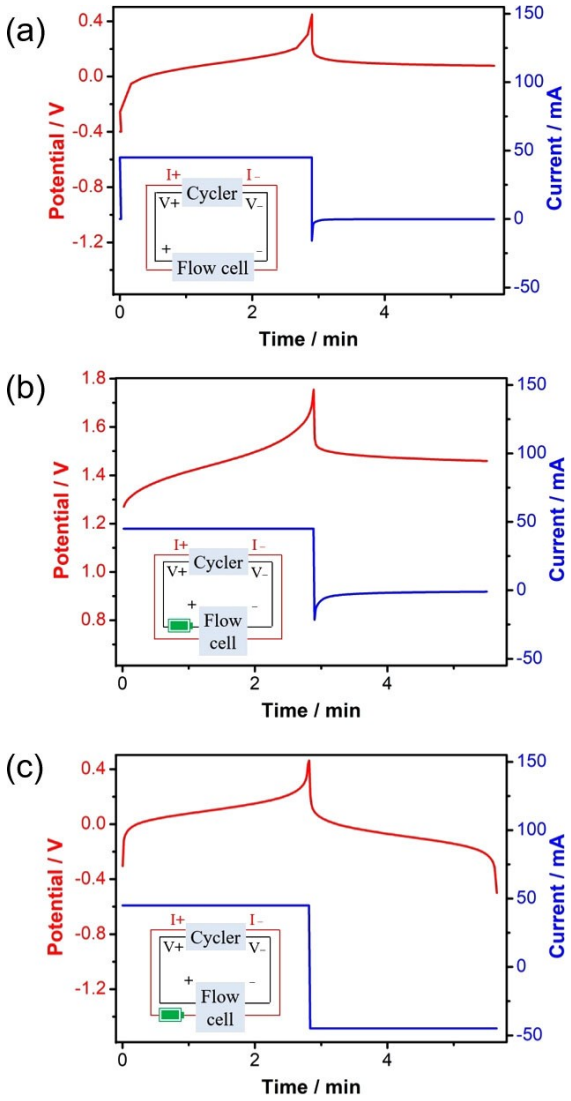

Figure 1. Symmetric redox static cell composed of 0.2 M ferro-/0.3 M ferricyanide in 1 M KCl (0.45 mL in CLS and NCLS) galvanostatically cycled at current densities of $\pm 15\ mA\,cm^{-2}$ with voltage cut-off values of ± 0.45 V. Time evolution of cell voltage and current for the three experimental setups shown schematically in the simplified diagrams: (a) cycler alone; (b) cycler with a Ni-MH battery incorporated in the voltage sense path; (c) cycler with a Ni-MH battery incorporated in the current path.

Interestingly, when the Ni-MH battery was included in the current path connecting the positive electrode of the static cell to the cycler (Figure 1c), the cell was successfully charged and discharged. That is, the proposed setup modification allows extending the cycler operational range to negative voltage values. Indeed, the cycling capability of the setup incorporating a Ni-MH battery in the current path is comparable to that of an Autolab PGSTAT12 potentiostat, as demonstrated by the identical galvanostatic cycling performance of the static ferro-/ferricyanide symmetric cell operated for 3 cycles with both systems, cycler and potentiostat (Figure 2). It is worth noting the remarkable overlap of the charge-discharge curves of the static ferro-/ferricyanide cell in the 3 consecutive cycles.

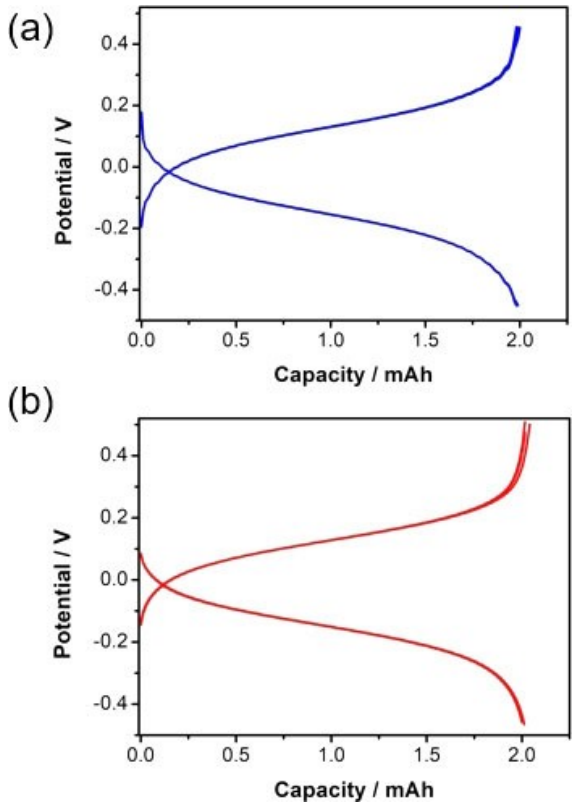

Figure 2. Symmetric redox static cell composed of 0.2 M ferro-/0.3 M ferricyanide in 1 M KCl (0.45 mL in each side) galvanostatically cycled at current densities of ±15 mA cm^{-2} with voltage cut-off values of ±0.45 V. Voltage-capacity profiles for 3 charge-discharge cycles performed with: (a) Neware cycler with a Ni-MH battery incorporated in the current path; (b) an Autolab PGSTAT12 potentiostat.

Advantages and disadvantages of the proposed setup

In addition to extending the strategy proposed by Aziz et al and allowing polarity reversing in battery tests with economic battery cyclers, the proposed setup has an additional benefit. Specifically, incorporating the Ni-MH battery in the current path allows monitoring directly the cell voltage without the voltage shifts introduced by batteries connected in the voltage sense path, as seen in Figure 1b. However, the method has an intrinsic drawback arising from incorporation of the Ni-MH in the current path. As current flows through the Ni-MH battery, its open circuit voltage (OCV) changes during flow cell operation, in clear contrast with Aziz's setup where the NiCd battery inserted in the voltage sense path remained always at a constant OCV since no current passed through the NiCd battery itself. That is, in our setup the Ni-MH gets charged and discharged during cell cycling. In our approach, the battery cell for charge compensation in the current circuit does not affect the cell voltage reading of the battery cycler, so that selection of the battery chemistry is not limited to those having flat voltage profiles such as Ni–Cd or Graphite – $LiFePO_4$. Among the mature, commercially available battery chemistries, Ni-MH was selected due to the following characteristics: i) it is aqueous based which is generally safe, ii) it can be slightly over-charged without major risks, iii) it operates well at high C-rates delivering high current densities, and iv) it possesses high lifespan when the depth of discharge is limited to 50% or below, in which Ni-MH batteries exceed 5.000 cycles.[15] It should be noted that the Ni-MH battery cell used in this work is able to operate well at 1 C (1000 mA), which translates to current density of 100 mA cm^{-2} for the system under evaluation (standard redox flow cell of 10 cm^2). Figure S2 shows the voltage profiles of a Ni-MH battery at 1000 mA (1 C) with and without a Ni-MH cell in the current line. There are no significant changes when the Ni-MH battery is added to the current line even at 1000 mA. Larger redox flow cells or high current densities may require the use of larger Ni-MH battery cells. Figure 3 shows representative cell voltage and OCV values of a Ni-MH battery plotted against time during galvanostatic cycling of a symmetric redox static cell (0.2 M ferro-/0.3 M ferricyanide in 1 M KCl, 0.45 mL in each side) at ±15 mA cm^{-2} with ±0.45 V cut-off voltage values using the experimental setup depicted schematically in Figure 1c. As can be seen, the OCV of the Ni-MH battery increases from 1.279 to 1.287 V during charging and decreases during discharging of the ferro-/ferricyanide cell, with a very stable and repetitive charge/discharge pattern over the 3 operated cycles. The OCV can be used to monitor the state of charge of the Ni-MH battery.

In order to assess the robustness and reliability of the proposed experimental setup over longer testing periods, the long-term cyclability of the ferro-/ ferricyanide static redox cell operated for 500 cycles with the cycler and one Ni-MH battery in the current path was explored. Galvanostatic charge-discharge curves of the static cell plotted every 100 cycles in Figure 4a indicate fairly stable performance, with 93.8% capacity retention after 500 cycles. Time evolution of the OCV of the Ni-MH battery during the 500 cycles (Figure 4b) reveals that the battery is also charging and discharging in each cycle, with its OCV value oscillating by 7–8 mV in each cycle. Overall, the OCV of the Ni-MH battery shifts with the number of cycles

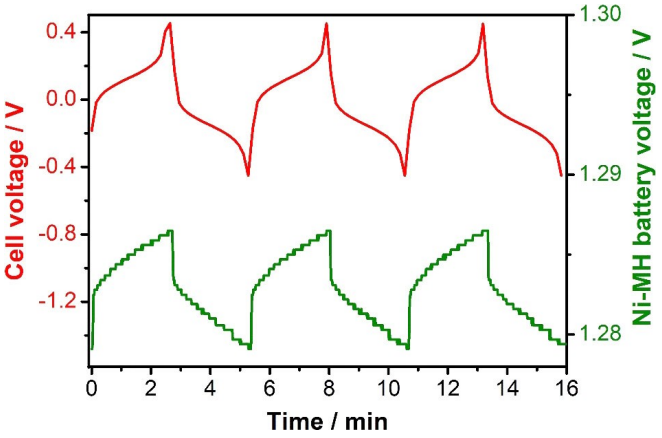

Figure 3. Evolution of cell voltage (top) and OCV of the Ni-MH battery (bottom) incorporated in the current path during galvanostatic cycling of a symmetric redox static cell (0.2 M ferro-/0.3 M ferricyanide in 1 M KCl, 0.45 mL in CLS and NCLS) at ±15 mA cm^{-2} current density and cut-off voltage values of ±0.45 V. Experimental setup depicted schematically in Figure 1c.

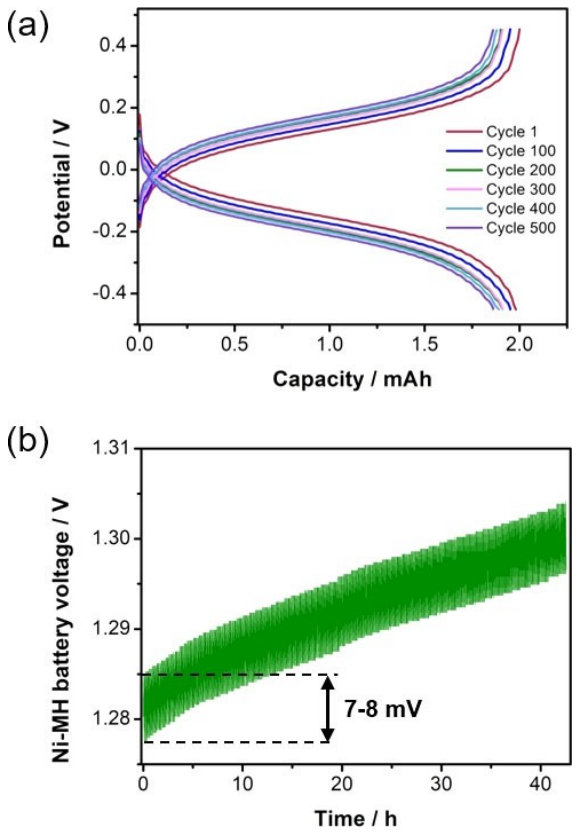

Figure 4. Long-term galvanostatic cycling (500 cycles) of a symmetric redox static cell (0.2 M ferro-/0.3 M ferricyanide in 1 M KCl, 0.45 mL in each side) at $\pm 15\ mA\,cm^{-2}$ with cut-off values of ± 0.45 V using a cycler with a Ni-MH battery incorporated in the current path. (a) Cell voltage-capacity profiles monitored every 100 cycles. (b) Time evolution of OCV of the Ni-MH battery during cycling.

with an average slope of $0.032\ mV\,cycle^{-1}$. That is, the Ni-MH battery required for long-term galvanostatic cycling of the symmetric redox cell becomes gradually charged during operation. However, such overcharging of the Ni-MH battery does not seem to have any impact on the cyclability of the ferro-/ferricyanide static redox cell, which exhibits comparable capacity retention to that typically obtained for the cell operated with a potentiostat.

Long-term cycling of a symmetric redox flow half-cell

In previous sections, the suitability of the proposed setup for extending the voltage capability of a Neware cycler has been validated with a symmetric redox cell under static (non-flow) configuration. It has been shown that long-term operation of such static cell increases the state of charge of the Ni-MH battery incorporated in the test setup, which nonetheless can be overcharged (float charged) unlike other battery types such as LIB. This makes it possible to continue cycling the static redox cell with an overcharged Ni-MH battery. In order to explore whether this applies also to operating redox flow symmetric cells, the capability of the experimental setup incorporating a Ni-MH battery that had been previously fully charged was tested for cycling a symmetric redox flow cell (0.2 M ferro-/0.2 M ferricyanide in 1 M KCl, 15 mL CLS and 50 mL NCLS). Prior to operating the redox flow cell, the Ni-MH battery was galvanostatically charged at 500 mA to a voltage of 1.48 V (100% SoC). Then the ferro-/ferricyanide symmetric redox flow cell was galvanostatically cycled at $\pm 10\ mA\,cm^{-2}$ current density with cut-off voltage values of ± 0.35 V at $40\ mL\,min^{-1}$ flow rate using the cycler with the fully-charged Ni-MH battery incorporated in the current path. Results shown in Figure 5 demonstrate that the experimental setup allowed stable cycling of the redox flow cell, as seen also for the redox static cell. Although the Ni-MH battery is fully-charged intentionally in the first charging cycle, the battery cycler is able to operate showing that overcharging of the Ni-MH is not limiting. It should be noted that overcharging does not pose safety concerns due to two facts. On the one hand, overcharging will be short, since the discharge process in the system under evaluation will decrease the state of charge of the Ni-MH. On the other hand, Ni-MH is an aqueous based system, which is safer than other battery chemistries such as Li-ion batteries. In particular, Ni-MH cells have in-cell charge control, which disconnects the charging current when overpressure is generated. In addition, Ni-MH cells contain a safety valve venting to release the gas. The evolution of the ferro-/ferricyanide cell voltage is very similar in all the charge-discharge cycles, illustrating the robustness of experimental setup using fully charged batteries. On the other hand, possible limitations arising from extremely low state of charge of the Ni-MH battery were also explored. A Ni-MH battery, which was intentionally discharged at 500 mA to a voltage of 0.8 V (fully discharged), was used to operate with the cycler the ferro-/ferricyanide symmetric redox flow cell galvanostatically at $\pm 10\ mA\,cm^{-2}$ with cut-off values of ± 0.35 V. It was found that the setup allowed charging the redox flow cell but was not capable of fully discharging it (Figure S1). The voltage of the pre-discharged Ni-MH battery decreased drastically from 1.33 V to

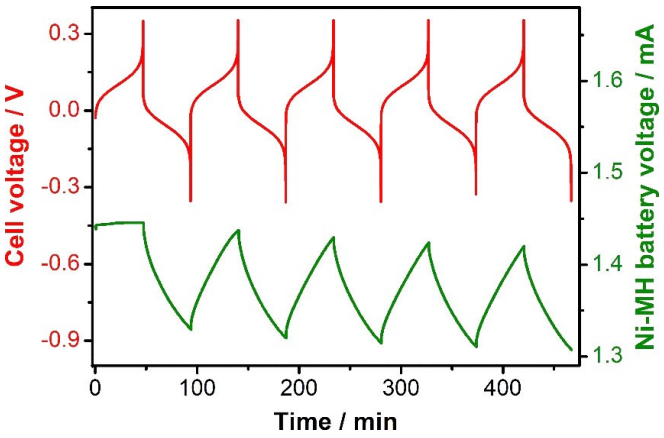

Figure 5. Time evolution of cell voltage (top) and OCV of a fully charged Ni-MH battery (bottom) incorporated in the current path during galvanostatic cycling of a symmetric redox flow cell (0.2 M ferro-/0.2 M ferricyanide in 1 M KCl, 15 mL CLS and 50 mL NCLS) at $\pm 10\ mA\,cm^{-2}$ with cut-off values of ± 0.35 V. It should be noted that the Ni-MH battery was fully charged intentionally.

0.43 V during the discharge step (Figure S1a, grey area) and the experimental setup with the discharged battery was not capable of sustaining the target discharge current density for the whole step (Figure S1b, grey area).

Lastly, the capability of the setup incorporating a Ni-MH battery at 50% SoC in the current path was investigated. Prior to operating the redox flow cell, the battery was brought to 50% SoC by discharging it at 500 mA to a voltage of 0.8 V and subsequently charging it at 550 mA for 1 h (nominal capacity of the Ni-MH battery was 1180 mAh). Long-term galvanostatic charge/discharge cycling (300 cycles) of the symmetric ferro-/ferricyanide redox flow cell (15 mL CLS and 50 mL NCLS) at $\pm 10\ mA\,cm^{-2}$ with cut-off values of ± 0.35 V was carried out with the cycler and the Ni-MH battery at 50% SoC incorporated in the current path. The redox flow cell operated with the setup exhibits a remarkable cycling stability, with measured discharge capacity (~77.7 mAh) and coulombic efficiency values (~99.6%) remaining fairly stable over the 300 charge/discharge cycles (> 19 days), as shown in Figure 6. Thus, we have demonstrated that a Ni-MH battery with a SoC ≈50% is required for long-term cycling of symmetric redox flow cells with the proposed experimental setup. It is worth noting that the theoretical capacity of the symmetrical flow cell to be tested should be considered when selecting the Ni-MH battery since the nominal charge capacity of the Ni-MH battery is recommended to be significantly larger than that of the symmetrical flow cell: 80 mAh for the flow cell versus 1180 mAh for the Ni-MH battery in our case. Indeed, a quick estimate of the required charge capacity of the Ni-MH battery (Eq. 1) should be conducted to ensure that the Ni-MH does not reach full state of charge during the experiment:

$$C_{NiMH} > 2 \times \left[\frac{C.I. \times C_{RFB}}{n}\right] \quad (1)$$

where C_{NiMH} is the charge capacity of the Ni-MH battery, C.I. and C_{RFB} are the coulombic inefficiency and the charge capacity of the redox flow battery under evaluation, respectively, and n is the expected number of cycles for the experiment.

In our case study, one Ni-MH battery cell of 1180 mAh was sufficient. Nevertheless, other experiment may require larger Ni-MH cells (e.g. 2200 mAh), or even several cells connected in parallel to ensure the required capacity.

To confirm that the cell voltage recorded in the battery cycler is due to changes in the redox potential of the electrolyte, we measured the potential of the CLS electrolyte solution on a separate channel of the cycler using a Pt wire and an Ag/AgCl reference electrode while operating the symmetric ferro-/ferricyanide redox flow cell (15 mL CLS and 50 mL NCLS) with the cycler and a Ni-MH battery in the current path. The flow cell was galvanostatically charged/discharged at $\pm 10\ mA\,cm^{-2}$ with cut-off voltage values of ± 0.35 V. The potential of the CLS electrolyte solution follows the same trends as the cell voltage during the charge/discharge steps, with values varying in the range between 0.15 and 0.42 V (vs. Ag/AgCl) as expected for the ferro-/ferricyanide redox pair (Figure S3).

After demonstrating the capabilities and limitations of the proposed setup for cycling symmetric redox flow cells, possible self-discharge of the ferro-/ferricyanide flow cell triggered by the Ni-MH battery inserted in the current path was explored. The cell was fully charged at $10\ mA\,cm^{-2}$ with cut-off voltage of +0.35 V, left at open circuit for different time periods (12 min, 24 h and 4 days) and then charged again to compare capacity with that of the initial charging step (79 mAh). Very small capacity values of ~ 0.1 mAh were obtained irrespective of the open-circuit step duration (Table S1), which accounts for only 0.13% of the initial charge capacity thus highlighting the absence of self-discharge in the tested timescale (up to 4 days).

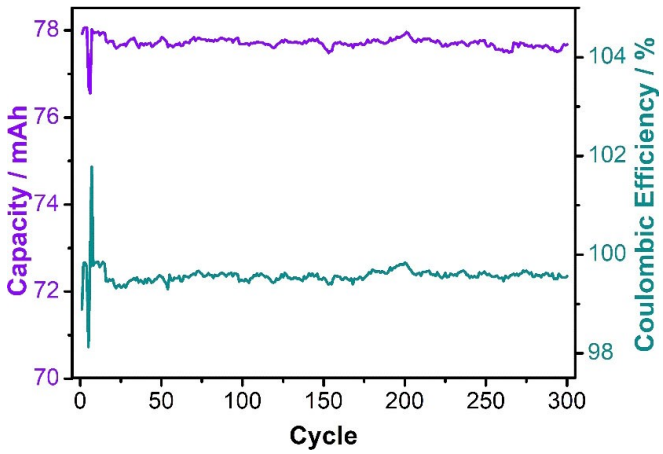

Figure 6. Discharge capacity (top) and coulombic efficiency (bottom) during long-term galvanostatic cycling (300 cycles > 19 days) of a symmetric redox flow cell (0.2 M ferro-/0.2 M ferricyanide in 1 M KCl, 15 mL CLS and 50 mL NCLS) at $\pm 10\ mA\,cm^{-2}$ with cut-off values of ± 0.35 V using a cycler with a Ni-MH battery at 50% SoC incorporated in the current path.

Extending setup capability for CCCV cycling

Next, we interrogated the capability of the proposed setup to conduct cycling tests by employing the constant current followed by constant voltage (CCCV) method. A symmetric redox static cell composed of 0.2 M ferro-/0.3 M ferricyanide in 1 M KCl (0.45 mL in both sides) was cycled at a constant current of $\pm 30\ mA\,cm^{-2}$, followed by constant charging and discharging voltages of 0.35 V and −0.35 V until the current dropped to $\pm 3.3\ mA\,cm^{-2}$. The first benchmark test was attempted with a Neware CT-4008T-5V6A-S1 cycler alone, without a Ni-MH battery incorporated in the circuit (Figure 7a), to show that the CC and CV can only be applied for charging the static redox cell, which cannot be discharged because negative current/voltages are outside the cycler's operational range (Figure 7b). To overcome this limitation, one Ni-MH battery was incorporated in the current path to operate the static redox cell using the CCCV method (Figure 7c). This setup allowed charging and discharging the ferro-/ferricyanide redox cell but only applying CC, not CV values (Figure 7d). This means that incorporating a Ni-MH battery in the current path enables tricking the system when it is operated in galvanostatic mode. As potentiostat (CV), the operating mode of the battery cycler changes and negative bias voltages cannot be applied. This limitation was addressed

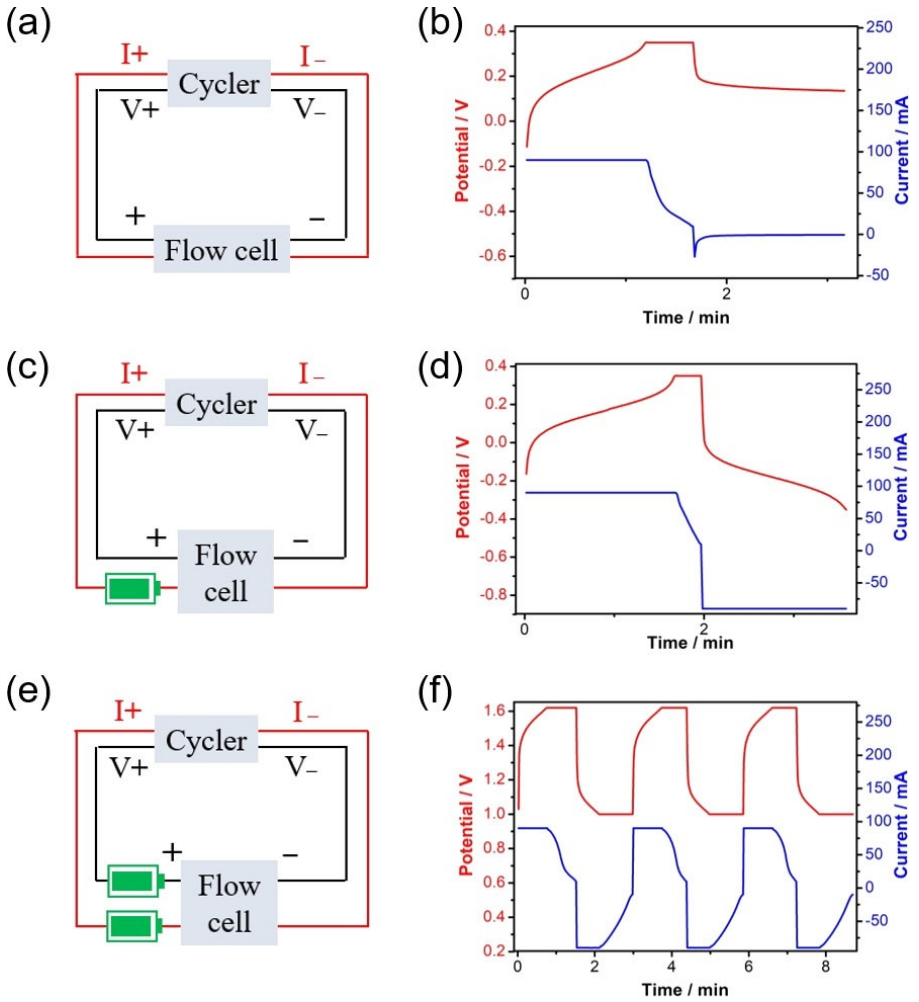

Figure 7. Symmetric redox static cell composed of 0.2 M ferro-/0.3 M ferricyanide in 1 M KCl (0.45 mL in CLS and NCLS) cycled using a CCCV protocol with $\pm 30\ mA\,cm^{-2}$ current density and cut-off values of ± 0.35 V followed by a constant charging/discharging voltage of ± 0.35 V until the current dropped to $\pm 3.3\ mA\,cm^{-2}$. Simplified schematic diagrams of the experimental setups and corresponding time evolution of cell voltage and current for: (a, b) cycler alone; (c, d) cycler with one Ni-MH battery (1.3 V) incorporated in the current path; (e, f) cycler with two Ni-MH batteries (1.3 V), incorporated in the voltage and the current paths, respectively.

by double-tricking the cycler using two Ni-MH batteries, one incorporated in the voltage path and another one in the current path connecting cycler and redox cell, as shown schematically in the simplified diagram in Figure 7e. This configuration allowed both charging and discharging the symmetric static redox cell using a CCCV method, with the redox cell exhibiting remarkable long-term cycling stability, as shown in Figure 7f for 3 representative charge/discharge cycles out of the total conducted ones (Figure S4). The application of CCCV enabled full charge/discharge step eliminating small differences in the depth of charge obtained in CC mode. As expected, incorporation of the battery in the voltage path resulted in the cell voltage shift sensed by the cycler reported by Aziz,[14] so that the recorded voltage value needs to be corrected by the OCV of the Ni-MH battery inserted in the voltage sensing path.

Implementation of the experimental setup in different battery cyclers

Finally, applicability of the experimental setup for galvanostatic cycling of a symmetric ferro-/ferricyanide redox static cell was explored in three additional battery cycler models. It was found that the working experimental setup for different battery cycler changes. The working configurations for each of the cyclers tested are indicated in Table 1 (with a tick) together with the associated effects in terms of measured cell voltage and changes in the OCV of the battery used to trick the battery cycler. Intriguingly, polarity reversing was achieved in some battery cyclers by incorporating the Ni-MH battery in the voltage path (the originally reported DC-offset approach) whereas other models required switching to the modified configuration, with the Ni-MH battery in the current path. In other cases, both configurations were valid. Lastly, battery cyclers having a single connecting cable to the redox cell worked by incorporating the battery in the only existing path.

Table 1. Working experimental setup for reversing polarity in electrochemical cell testing with different battery cyclers and associated effects.

Cycler	Working setup configuration		Associated effect
	Battery in voltage path	Battery in current path	
Neware CT-4008T-5V6A-S1	x	√	Actual cell voltage measured OCV of the incorporated Ni-MH battery changes
Neware CT-4008Tn-5V6A-S1-F	√	√	Configuration-dependent
Maccor Series 4000	√ Only one path		Shift in measured cell voltage OCV of the incorporated Ni-MH battery changes
Biologic BCS-805	√	x	Shift in measured cell voltage Battery OCV remains constant

That is, these few examples illustrate how the working experimental setup for extending the cycler capability to negative voltage values has to be explored and tested in a case-by-case basis.

Conclusions

Extending the simple and inexpensive methodology for reversing polarity in electrochemical cell testing (referred as "the poor academic's DC-offset approach") to other battery cyclers unraveled an unexpected failure for a certain battery cycler model (Neware CT-4008T-5V6A-S1). A modification of the experimental setup was proposed here for those battery cyclers where the reported DC-offset approach could not be implemented, hence broadening its applicability to more electrochemical cell testing systems. In the modified setup, a Ni-MH battery was incorporated in the path of the current cable connecting electrochemical cell and battery cycler, whereas in the original method the cycler was "tricked" by incorporating the battery in the path of the battery cycler's voltage sense. The suitability of the proposed approach was demonstrated for long-term cycling of symmetric ferro-/ferricyanide redox cells under static and flow configuration using both galvanostatic and potentiostatic methods. While the proposed setup modification successfully allowed extending the cycler operational range to negative bias voltage values during cycling of symmetric ferro-/ferricyanide redox cells, its specific configuration had intrinsic advantages and limitations. Thus, incorporating the Ni-MH battery in the current path allowed direct monitoring of the cell voltage without the voltage shifts introduced by batteries connected in the voltage sense path. However, as current flowed through the Ni-MH battery, it became charged and discharged during flow cell cycling. Tests with the Ni-MH battery at different states of charge indicated that a SoC $\geq$ 50% was required for long-term cycling of symmetric redox flow cells with the proposed experimental setup. The symmetric flow cell charged with the setup showed negligible self-discharge after long times left at open circuit. Incorporation of an additional Ni-MH battery in the voltage path was needed to implement a CCCV cycling protocol with negative current densities and voltage values. Tailored experimental setups to reverse polarity in electrochemical cell cycling were provided for four types of battery cyclers, thus contributing to broaden the applicability of the useful methodology for poor academics.

Experimental Section

Materials. All reagents and solvents were analytical grade and used as received without further purification. Potassium ferrocyanide trihydrate and potassium ferricyanide were purchased from Thermoscientific and potassium chloride from Aldrich. Solutions were prepared using deionized water.

Cell experiments. A filter-pressed flow cell using Nafion 212 (Ion Power) and graphite felt (SGL) as the ion selective membrane and electrodes was used for the flow experiments. Graphite felt was thermally activated at 400 °C for 2 days. The projected area of the cell was 10 cm^2 and the flow rate was fixed at ca. 40 mL min^{-1}. General conditions for the flow cell: Capacity limiting side (CLS): 15 mL of 0.2 M $K_4[Fe(CN)_6]$ in 1.0 M KCl; non-capacity limiting side (NCLS): 50 mL of 0.2 M $K_3[Fe(CN)_6]$ and 0.1 M $K_4[Fe(CN)_6]$ in 1.0 M KCl. In some experiments, a smaller area (3 cm^2) filter-pressed cell with the same components but operating under non-flow or static configuration (without external tanks) was used. General conditions for the static cell: CLS (0.45 mL), 0.2 M $K_4[Fe(CN)_6]$ in 1.0 M KCl; NCLS (0.45 mL), 0.3 M $K_3[Fe(CN)_6]$ in 1.0 M KCl.

Electrochemical Characterization: Galvanostatic charge–discharge measurements were performed using different battery testing systems (BTS), specifically Neware BTS models CT-4008T-5V6A-S1 and CT-4008Tn-5V6A-S1-F, a Maccor Series 4000 and a Biologic BCS-805. The ferro/ferricyanide symmetric cells were galvanostatically charged/ discharged at current densities of $\pm$15 mA cm^{-2} with voltage limits at $\pm$0.45 V (static cell) and at $\pm$10 mA cm^{-2} with voltage limits at $\pm$0.35 V (flow cell). Comparative cycling tests were performed using an Autolab PGSTAT12 potentiostat (Methrom-Autolab, The Netherlands) with NOVA 2.1.3 software. Cycling tests of ferro/ferricyanide symmetric cells were also conducted by employing the constant current followed by constant voltage (CCCV) protocol, applying a constant current density of $\pm$30 mA cm^{-2} with cut-off values of $\pm$0.35 V, followed by a constant charging/discharging voltage of $\pm$0.35 V until the current dropped to $\pm$3.3 mA cm^{-2}. The potential of the CLS electrolyte solution was measured with a separate channel of the cycler using a Pt wire and an Ag/AgCl reference electrode (BioLogic).

In order to extend the cycler's operational voltage range, Panasonic AA Ni-MH batteries (1.2 V, 1.18 Ah) were incorporated in the current path connecting the cycler and flow cell (red lines in the circuit diagram shown in Figure 1). The OCV of the NiMH was measured using a separate channel of the cycler.

Acknowledgements

The authors acknowledge financial support by the Spanish Government (Ministerio de Ciencia e Innovacion, Grants PID2021-124974OB-C22 and TED2021-131651B-C21) and Ramon y Cajal award (RYC2018-026086-I) as well as the MeBattery project. MeBattery has received funding from the European Innovation Council of the European Union under Grant Agreement no. 101046742. This work was supported by the Regional Government of Castilla y Leon (Junta de Castilla y Leon), the Basque Government (GV-ELKARTEK-2022 KK-2022/00043) and by the Ministry of Science and Innovation MICIN and the European Union NextGeneration EU/PRTR (C17. I1). Gimena Marin is supported by a grant from the Regional Government of Castilla y León (Junta de Castilla y León), which is partially supported by the European Social Fund.

Conflict of Interests

The authors declare no conflict of interest.

Data Availability Statement

The data that support the findings of this study are available from the corresponding author upon reasonable request. In addition, dataset of the raw data will be made available in the public repository Zenodo.

Keywords: Battery cycler · electrochemistry · redox flow battery · reversing polarity · symmetrical cell

[1] E. Sánchez-Díez, E. Ventosa, M. Guarnieri, A. Trovò, C. Flox, R. Marcilla, F. Soavi, P. Mazur, E. Aranzabe, R. Ferret, *J. Power Sources* **2021**, *481*, 228804.
[2] G. L. Soloveichik, *Chem. Rev.* **2015**, *115*, 11533–11558.
[3] A. A. Kebede, T. Kalogiannis, J. Van Mierlo, M. Berecibar, *Renewable Sustainable Energy Rev.* **2022**, *159*, 112213.
[4] C. Choi, S. Kim, R. Kim, Y. Choi, S. Kim, H. Jung, J. H. Yang, H.-T. Kim, *Renewable Sustainable Energy Rev.* **2017**, *69*, 263–274.
[5] 2022 Final List of Critical Minerals. Department of the Interior, U.S. Government, 2022.
[6] Study on the Critical Raw Materials for the EU 2023. European Commission, 2023.
[7] Z. Li, T. Jiang, M. Ali, C. Wu, W. Chen, *Energy Storage Mater.* **2022**, *50*, 105–138.
[8] a) F. Zhong, M. Yang, M. Ding, C. Jia, *Front. Chem.* **2020**, *8*, 451; b) Z. Li, Y. C. Lu, *Adv. Mater.* **2020**, *32*, 2002132.
[9] Y. Yao, J. Lei, Y. Shi, F. Ai, Y. C. Lu, *Nat. Energy* **2021**, *6*, 582–588.
[10] J. D. Milshtein, A. P. Kaur, M. D. Casselman, J. A. Kowalski, S. Modekrutti, P. L. Zhang, N. Harsha Attanayake, C. F. Elliott, S. R. Parkin, C. Risko, F. R. Brushett, S. A. Odom, *Energy Environ. Sci.* **2016**, *9*, 3531–3543.
[11] T. Páez, A. Martínez-Cuezva, R. Marcilla, J. Palma, E. Ventosa, *J. Power Sources* **2021**, *512*, 230516.
[12] M.-A. Goulet, M. J. Aziz, *J. Electrochem. Soc.* **2018**, *165*, A1466–A1477.
[13] a) E. Ventosa, *Curr. Opin. Chem. Eng.* **2022**, *37*, 100834; b) T. Páez, A. Martínez-Cuezva, J. Palma, E. Ventosa, *ACS Appl. Energ. Mater.* **2019**, *2*, 8328–8336.
[14] K. Amini, E. M. Fell, M. J. Aziz, *J. Electrochem. Soc.* **2022**, *169*, 090527.
[15] a) X. Chen, A. Chu, D. Li, Y. Yuan, X. Fan, Y. Deng, *J. Energy Storage* **2021**, *32*, 101999; b) M. Brady, *Assessment of Battery Technology for Rail Propulsion Application*, United States Federal Railroad Administration, **2017**.

Manuscript received: October 2, 2023
Revised manuscript received: November 16, 2023
Version of record online: December 13, 2023